

Determination of the Energized State Operating Point of an AC Contactor Coil Using a Bayesian Neural Network

Son T. Nguyen*, Tu M. Pham, Anh Hoang, Tu A. Nguyen

Hanoi University of Science and Technology, Ha Noi, Vietnam

*Corresponding author email: son.nguyenthanh@hust.edu.vn

Abstract

The paper presents a method for determining the energized operating point of an AC contactor coil using the finite element method (FEM) combined with a Bayesian neural network (BNN) model. Under actual operating conditions, the magnetic flux density and air-gap length of the electromagnet directly influence the electromagnetic force within the contactor and, consequently, the overall device performance. However, these quantities are difficult to measure accurately in practice. The objective of this study is to propose a computational approach for estimating the magnetic flux density and air-gap length of the contactor by integrating machine learning techniques with FEM simulations. The proposed method establishes an electromagnetic model of the contactor coil, in which the magnetic flux density varies from 1.0 T to 1.5 T and the air-gap length ranges from 0.05 mm to 0.30 mm, generating the corresponding voltage drops across the coil. The simulated dataset is then used to train a BNN in an inverse inference direction, enabling prediction of the magnetic flux density and air-gap length from a known operating voltage. Based on these estimated quantities, the electromagnetic attraction force is calculated using FEM, facilitating analysis of the contactor's operating characteristics and providing a foundation for design optimization in industrial applications.

Keywords: AC contactor coil, bayesian neural network, finite element method.

1. Introduction

In modern industrial electrical systems, switching devices are essential components responsible for the reliable connection and disconnection of electrical circuits, as well as for ensuring protection against abnormal operating conditions or electrical faults. These devices enable safe control of power flow, automation of processes, and protection of equipment from damage caused by overloads or short circuits. Among the various types of switching devices, the AC contactor stands out as a fundamental electromagnetic switch that is extensively employed in industrial and commercial applications. It is primarily used for controlling, protecting, and switching high-power electrical loads, such as motors, heating systems, and lighting circuits. By providing remote and automatic control of power circuits, AC contactors enhance both the efficiency and safety of modern electrical installations.

During continuous operation, mechanical wear and electrical stresses—such as arcing, contact erosion, and material degradation—gradually accumulate in AC contactors, leading to increased contact resistance, reduced switching performance, and potential loss of contact integrity. As deterioration progresses, the device may exhibit delayed response, incomplete closure, or even total failure. Consequently, numerous studies have focused on accurately assessing and predicting the reliability and remaining electrical life of AC contactors.

These efforts aim to clarify degradation mechanisms, model aging behaviour, and develop predictive maintenance strategies to detect potential failures in advance, thereby improving system reliability, safety, and operational continuity while minimizing downtime and maintenance costs [1-3].

Over the past decades, the finite element method (FEM) has been widely employed to simulate the electromagnetic and mechanical characteristics of various electromagnetic devices. In [4], a two-dimensional (2D) FEM model was developed that integrates electromagnetic field analysis, transient electrical circuit modelling, and the mechanical motion of the armature, enabling the simulation of the dynamic behaviour of AC contactors during coil excitation. The FEM approach provides a reliable means of accurately predicting the operating performance of the contactor coil, with simulation results showing strong agreement with experimental measurements.

The operating characteristics of an AC contactor coil are strongly influenced by key electromagnetic parameters, particularly the magnetic flux density and the length of the air gap within the magnetic circuit. These quantities directly determine the magnitude of the electromagnetic attraction force generated by the contactor's electromagnet, which governs the closing dynamics, response time, and stability of the armature movement. Accurate estimation of these parameters is

therefore essential for ensuring high operating efficiency, reliable switching performance, and extended service life of the device. However, under real operating conditions, direct measurement of magnetic flux density and air-gap variations is extremely difficult. The installation of sensors within the confined structure of the electromagnetic mechanism is limited by space constraints, harsh electromagnetic interference, and the risk of altering the device's behavior. Additionally, the fast transient nature of switching events further complicates measurement. These practical challenges motivate the development of advanced modeling, estimation, and signal-based diagnostic techniques capable of capturing these internal parameters without intrusive access to the system.

Full-scale finite element method (FEM) simulations often demand substantial computation time, particularly when performing parameter sweeps or multi-condition analyses. In modern industrial systems, where computational efficiency and real-time responsiveness are crucial, the integration of FEM with machine learning techniques has emerged as a promising solution [5, 6]. Among these approaches, artificial neural networks (ANNs) have demonstrated strong potential, as they can learn the complex nonlinear relationships between electrical signals (e.g., voltage and current) and mechanical quantities (e.g., armature displacement and electromagnetic force) in AC contactors. This capability enables accurate prediction of device behaviour without relying on time-intensive FEM simulations.

Bayesian neural networks (BNNs) are an advanced extension of traditional artificial neural networks. Unlike conventional models that treat network weights and biases as fixed parameters, BNNs represent them as probability distributions, enabling the model to naturally capture prediction uncertainty [7]. Through Bayesian inference, these distributions are updated based on observed data, resulting in a posterior distribution over the network parameters. Predictions are then obtained by averaging over this posterior, providing both output values and associated confidence estimates. BNNs offer key advantages such as uncertainty quantification, improved generalization on small or noisy datasets, robustness in the presence of incomplete data, and the ability to incorporate prior knowledge into the learning process. These features make BNNs particularly useful in safety-critical or data-limited applications.

In this study, the dataset for BNN training was generated using the electromagnetic model of a commercial AC contactor, simulated with Finite Element Method Magnetics (FEMM) [8], an open source 2D FEM tool for magnetostatic and electromagnetic analysis. In the simulations, the magnetic flux density in the air gap was varied from 1.0 T to 1.5 T, while the air-gap length was swept from 0.05 mm to 0.30 mm. The coil current was measured experimentally and used as the input to the FEM-based model, from which the corresponding coil voltage was

obtained. The resulting dataset was then used to train a BNN capable of mapping coil voltage to flux density and air-gap length, thereby enabling the estimation of the contactor's operating condition directly from voltage measurements.

The main innovation of this study is its ability to estimate key internal parameters of AC contactors, including magnetic flux density and air-gap length, without the need for intrusive sensors or computationally expensive full FEM simulations.

By combining experimentally measured coil current with FEM-generated data to train a BNN, the proposed approach enables fast, accurate, and uncertainty-aware estimation directly from coil voltage measurements. This non-invasive method simplifies measurement, enhances reliability, and supports real-time monitoring and predictive maintenance of industrial switching devices.

The remainder of this paper is structured as follows. Section 2 briefly describes the construction and operation of AC contactors. Section 3 introduces Finite Element Method Magnetics (FEMM) as an effective 2D FEM tool for analysing their electromagnetic behaviour. Section 4 presents the concept of BNNs for regression applications. Section 5 explains the determination of the operating point of the energized AC contactor coil. Section 6 outlines the experimental setup for measuring electrical parameters and the procedure used to estimate the operating point. Finally, Section 7 concludes the study.

2. Construction and Operation of AC Contactors

An AC contactor, as shown in Fig. 1, consists of several key components that work together to control the switching of electrical circuits. The coil (solenoid winding) generates a magnetic field when energized by an AC supply, which produces the force needed to move the armature. The magnetic core (fixed iron core), usually made of laminated soft iron, provides a low-reluctance path for the magnetic flux and directs it toward the movable part. The armature (moving iron core) is attracted to the fixed iron core when the coil is energized, causing the contacts to close and complete the electrical circuit.

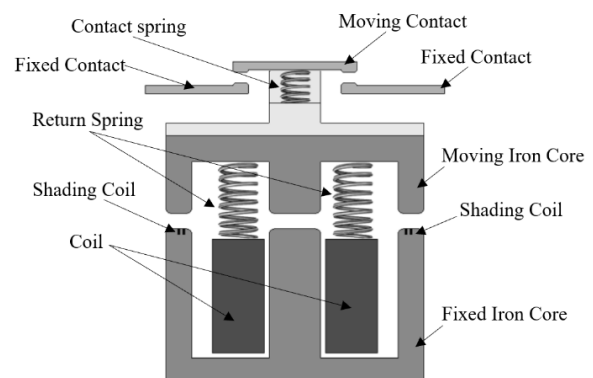


Fig. 1. Key components of an AC contactor

Two shading coils, small copper rings placed on two pole faces, are used to create a phase-shifted magnetic flux that prevents armature vibration. The contacts, divided into main and auxiliary types, are responsible for carrying the large current and performing control or signaling functions, respectively. A spring returns the armature to its original position when the coil is de-energized, ensuring the contacts open quickly and safely. Finally, the frame and housing provide structural support, electrical insulation, and protection for all internal components, ensuring reliable and durable operation.

When the AC supply is applied to the coil, an alternating magnetic field is produced in the magnetic core. The magnetic flux induces an electromagnetic force that attracts the armature. The magnitude of this force depends on the coil current, the number of turns of the coil, the magnetic permeability of the core material, and the air gap between the armature and the core. The electromagnetic force can be computed as follows:

$$F = \frac{B^2 A}{2\mu_0} = \frac{\mu_0 (NI)^2 A}{2g^2} \quad (1)$$

where

- F : Electromagnetic force (N),
- B : Magnetic flux density (T),
- A : Cross-sectional area of the core (m^2),
- μ_0 : Permeability of free space ($4\pi 10^{-7} H / m$),
- N : Number of turns of the coil,
- I : Current through the coil,
- g : Air-gap distance between armature and core (m).

Number of turns can be determined as follows:

$$N = \frac{V}{4.44 f B_m A} \quad (2)$$

where

- V : Root-mean-square (RMS) voltage of the coil,
- f : Frequency (Hz),
- B_m : Maximum flux density (T),
- A : Core cross-sectional area (m^2).

3. Electromagnetic Analysis of AC Contactors Using Finite Element Method Magnetics

The FEM is a powerful numerical technique used to solve complex electromagnetic field problems that are difficult or impossible to address analytically. In FEM, the geometry of a device is divided into many small,

discrete regions called elements, over which the governing field equations are approximated. By assembling the solutions of all elements, FEM provides an accurate approximation of the overall electromagnetic behavior of the system. This method is widely employed in the design, analysis, and optimization of electrical machines, transformers, actuators, sensors, and other electromagnetic devices, enabling engineers to predict performance, identify potential issues, and improve efficiency before physical prototyping.

In this study, electromagnetic analyses of an AC contactor were performed using FEMM, which allows accurate computation of the magnetic flux density, field distribution, and electromagnetic force as functions of coil excitation and air-gap length. FEMM can solve simplified forms of Maxwell's equations, depending on the type of problem-magnetostatic, harmonic, or electrostatic.

FEMM provides multiple advantages over commercial platforms such as ANSYS, particularly in academic and research settings. Unlike ANSYS, FEMM is completely free, lightweight, and does not require expensive licenses or high-end computing hardware, which makes it highly accessible for researchers and educators. Its interface is straightforward and well-suited for 2D planar and axisymmetric problems, enabling fast model creation and efficient numerical computation. In addition, FEMM offers built-in Lua scripting capabilities that support automated parametric simulations, batch processing, and seamless interaction with external tools such as MATLAB, Octave, and machine-learning frameworks. These features allow flexible customization and efficient data generation, which are essential for developing and training predictive models. As a result, FEMM serves as a practical, user-friendly platform for electromagnetic device modeling when rapid simulation, low computational cost, and integration with external algorithms are required.

The core Maxwell's equations implemented in FEMM are as follows:

$$\nabla \cdot D = \rho \quad (3)$$

$$\nabla \cdot B = 0 \quad (4)$$

$$\nabla \times E = -\frac{\partial B}{\partial t} \quad (5)$$

$$\nabla \times H = J + \frac{\partial D}{\partial t} \quad (6)$$

where

- E : Electric field intensity (V / m),
- $D = \epsilon E$: Electric flux density (C / m^2),
- H : Magnetic field intensity (A / m),

- $B = \mu H$: Magnetic flux density (T),
- J : Current density (A / m^2),
- C : Charge density (C / m^3).

The FEM-based analysis model of the AC contactor is primarily based on the equations governing time-harmonic (AC) magnetic problems, as follows:

$$\nabla \times \left(\frac{1}{\mu} \nabla \times A \right) = j\omega\sigma A - J_s \quad (7)$$

where

- ω : Angular frequency (rad / s),
- σ : Conductivity (S / m),
- J_s : Source current density (A / m^2).

By using FEMM, it is possible to analyze the influence of parameters such as coil current, air-gap variation, and core geometry on the electromagnetic characteristics of the AC contactor. The following parameters of the AC contactor coil can be determined: the resistance, reactance, and electromagnetic force.

4. Bayesian Neural Networks

BNNs are a type of artificial neural networks (ANNs) that incorporate Bayesian inference to handle uncertainty in network parameters (weights and biases). Instead of assigning fixed values to the weights, BNNs treat them as probability distributions, enabling the network to make probabilistic predictions.

According to Bayes' theorem, the inference equation can be expressed as follows:

$$p(w|D) = \frac{p(D|w)p(w)}{p(D)} \quad (8)$$

where

- $p(w|D)$: The posterior distribution of weights and biases in the network,
- $p(D|w)$: The data likelihood (how likely the data is given the weights and biases),
- $p(w)$: The prior distribution of weights and biases in the network,
- $p(D)$: The evidence.

In Bayesian inference for neural networks, the hyperparameters of the cost function, such as prior variances, regularization terms, or noise levels, are not set arbitrarily but are determined according to the principle of maximum evidence. This principle, also known as type-II maximum likelihood, involves selecting hyperparameters that maximize the marginal likelihood of the observed data, integrating over all possible network weights. By doing so, the network automatically balances model complexity and data fit,

leading to more robust learning, improved generalization, and principled handling of uncertainty in predictions.

BNNs usually consist of three layers as follows:

- The input layer receives the input data (features),
- The hidden layer performs computations and extracts relationships or patterns,
- The output layer produces the result or decision.

4.1. Forward Propagation

First, the input values to the network are denoted by x_i where $i = 1, \dots, d$. The activation of the hidden layer is as follows:

$$a_j^{(1)} = \sum_{i=1}^d w_{ji}^{(1)} x_i + b_j^{(1)} \quad j = 1, \dots, M \quad (9)$$

where

- $w_{ji}^{(1)}$: Weight on the connection from the i -th input to the j -th hidden node,
- $b_j^{(1)}$: Bias of the j -th hidden node,
- $a_j^{(1)}$: Activation of the j -th hidden node,
- d : Number of inputs,
- M : Number of hidden nodes.

The activation of the hidden layers is then used to compute the outputs of hidden nodes as follows:

$$y_j^{(1)} = f_1(a_j^{(1)}) \quad j = 1, \dots, M \quad (10)$$

where $f_1(\cdot)$ is the activation function of the hidden layer, which is a 'tanh' function as follows:

$$y_j^{(1)} = \tanh(a_j^{(1)}) \quad (11)$$

The activation function of the hidden layer has the following properties:

$$\frac{\partial y_j}{\partial a_j} = 1 - y_j^2 \quad (12)$$

The activations of output nodes are computed as follows:

$$a_k^{(2)} = \sum_{j=1}^M w_{kj}^{(2)} y_j + b_k^{(2)} \quad k = 1, \dots, c \quad (13)$$

where

- $w_{kj}^{(2)}$: Weight on the connection from the j -th hidden node to the k -th output node,
- $b_k^{(2)}$: Bias of the k -th output node,

- $a_k^{(2)}$: Activation of the k -th output node,
- c : Number of output nodes.

For regression problems, the linear function is used for the activation of output nodes, which is as follows:

$$z_k = a_k^{(2)} \quad (14)$$

4.2. Cost Function

The BNN training requires the definition of a cost function, which has the following form:

$$S = \beta E_D + \alpha E_W \quad (15)$$

where E_D is the sum-of-square error function as follows:

$$E_D = \frac{1}{2} \sum_{n=1}^N \sum_{k=1}^c \{z_k(x_n; w) - t_{nk}\}^2 \quad (16)$$

where

- N : Number of patterns in the training data,
- x_n : The n -th input data,
- t_n : The n -th target data corresponding to the k -th output,
- w : Vector of weights and biases in the network.

In (15), β represents the constant inverse variance and α denotes the regularization constant that penalizes large weights and biases, thereby mitigating the overfitting phenomenon in the network after training. E_D is also called the data error function. β and α are also called ‘hyperparameters’. E_W is called the weight function, which is given by:

$$E_W = \frac{1}{2} \|w\|^2 = \sum_{i=1}^W w_i^2 \quad (17)$$

where W is the number of weights and biases in the network. β and α can be automatically determined using the Bayesian inference. At the most probable vector of weights and biases, w_{MP} , the relationship between E_W^{MP} and α is as follows:

$$2\alpha E_W^{MP} = W - \sum_{i=1}^W \frac{\alpha}{\lambda_i + \alpha} \quad (18)$$

where λ_i ($i = 1, \dots, W$) are the eigenvalues of the Hessian matrix of the data error, E_D . The right-hand side of (18) is equal to a value γ defined as follows:

$$\gamma = \sum_{i=1}^W \frac{\lambda_i}{\lambda_i + \alpha} \quad (19)$$

From (18) and (19), the value of α can be computed

as follows:

$$\alpha = \frac{\gamma}{2E_W^{MP}} \quad (20)$$

At the most probable vector of weights and biases, w_{MP} , the relationship between E_D^{MP} and β is as follows:

$$2\beta E_W^{MP} = N - \sum_{i=1}^W \frac{\lambda_i}{\lambda_i + \alpha} = N - \gamma \quad (21)$$

From (21), the value of β can be calculated as follows:

$$\beta = \frac{N - \gamma}{2E_W^{MP}} \quad (22)$$

Equations (19), (20) and (22) are used to update the values of α and β during the network training process.

4.3. Update of Weights and Biases

The vector of the network weights and biases can be updated via an iterative process as follows:

$$w[k+1] = w[k] + \eta[k] d[k] \quad (23)$$

where

- $w[k]$: Vector of weights and biases at the k -th iteration,
- $w[k+1]$: Vector of weights and biases at the k -th iteration,
- $d[k]$: Search direction at the k -th iteration,
- $\eta[k]$: Learning rate at the k -th iteration.

The vector of weights and biases are updated to minimize the difference between the predicted and actual outputs. This is done through training algorithms, typically using a method called backpropagation, combined with an optimization algorithm such as the scaled conjugate gradient method [9].

The BNN training procedure includes the following steps.

- **Step 1:** Initialize the values for α and β . The network weights and biases are initialized from the prior distribution defined for α .
- **Step 2:** Update the vector of the network weights and biases to minimize the cost function, S .
- **Step 3:** When the cost function has reached a local minimum, the values of α and β can be re-estimated as follows:

$$\alpha_{new} = \frac{\gamma_{old}}{2E_W} \quad (24)$$

$$\beta_{new} = \frac{N - \gamma_{old}}{2E_W} \quad (25)$$

- **Step 4:** Repeat Steps 2 and 3 until convergence is reached.

5. Determination of the Energized State Operating Point of the AC Contactor Coil

FEMM is used to simulate the electromagnetic behavior of the AC contactor coil under different excitation conditions, illustrating how the magnetic flux density and air-gap length vary with the applied voltage. A BNN is then employed to estimate the magnetic flux density and air-gap length at the energized-state operating point of the AC contactor coil. Let B_m in the range of 1 to 1.5T represent the vector of magnetic flux density values and g in the range of 0.05 to 0.5 mm represent the vector of corresponding air-gap lengths. These vectors form the dataset used for BNN training. The magnetic flux density values were discretized with an increment of 0.05 (T), covering the full range from the minimum to the maximum observed limits. Similarly, the air-gap length values were sampled at steps of 0.05 (mm) across their entire operating range. Based on these step resolutions and limits, a total of 110 distinct data patterns were generated for the dataset.

The input and target variables used for training the BNN are organized as follows.

- Input: the applied coil voltage of the AC contactor,
- Targets: the corresponding magnetic flux density and air-gap length.

Based on this configuration, the BNN architecture consists of one input node, ten hidden nodes (which may be adjusted depending on the training performance), and two output nodes representing the predicted magnetic flux density and air-gap length.

Once trained, the BNN establishes a direct mapping from the measured applied voltage to the estimated electromagnetic parameters of the AC contactor. By predicting the magnetic flux density and air-gap length and using the experimentally measured coil current, several key parameters of the energized coil can be determined:

- Voltage drops across the coil,
- Coil resistance,
- Coil reactance,
- Instantaneous electromagnetic force.

This approach eliminates the need for direct measurement of these internal parameters, enabling

efficient and non-intrusive evaluation of the contactor's operating condition.

6. Experiment

This section describes the procedure used to set up the experimental system for measuring the electrical parameters of an AC contactor coil. The complete arrangement is shown in Fig. 2, which illustrates the method used to acquire both the voltage applied to the coil and the current flowing through it. The experimental system is designed to accurately capture real-time electrical signals while ensuring safe and reliable operation. The setup consists of the following components:

- Voltage and current sensors, used to measure the instantaneous coil voltage and current waveforms,
- A National Instruments USB-6009 data acquisition (DAQ) device, which converts the analog sensor outputs into digital signals suitable for processing,
- A laptop running a graphical user interface (GUI)-based DAQ software, used for real-time signal monitoring, data recording, and export of measurement results for further analysis.

Together, these components form an integrated measurement system capable of capturing coil behavior under energized operating conditions, providing the necessary data for subsequent parameter estimation and BNN-based prediction.

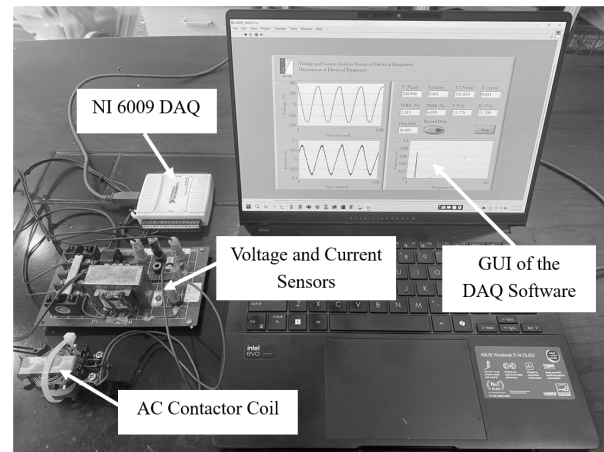


Fig. 2. The experimental system

Fig. 3 shows the graphical user interface (GUI) of the DAQ software, which provides real-time monitoring and visualization of the electrical quantities measured from the AC contactor coil. The software displays the following parameters:

- Waveform of the applied voltage,
- Waveform and fast Fourier transform (FFT) of the coil current,
- RMS value of the voltage,

- RMS value of the current,
- Total harmonic distortion (THD) of the voltage,
- THD of the current.

In addition, Fig. 4 illustrates typical examples of the voltage waveform, current waveform, and their corresponding FFT analyses obtained from the measurement system. The DAQ software also enables the user to record these waveforms for offline evaluation and post-processing. From the recorded voltage and current data, RMS values of the voltage and current can be computed as follows:

$$V_{RMS} = \sqrt{\frac{1}{N} \sum_{i=1}^N V_i^2} \quad (26)$$

$$I_{RMS} = \sqrt{\frac{1}{N} \sum_{i=1}^N I_i^2} \quad (27)$$

where

- V_{RMS} : RMS value of the voltage,
- I_{RMS} : RMS value of the current,
- V_i : Value of the voltage at the i -th sampling instant,
- I_i : Value of the current at the i -th sampling instant,
- N : Number of samples of the voltage and current.

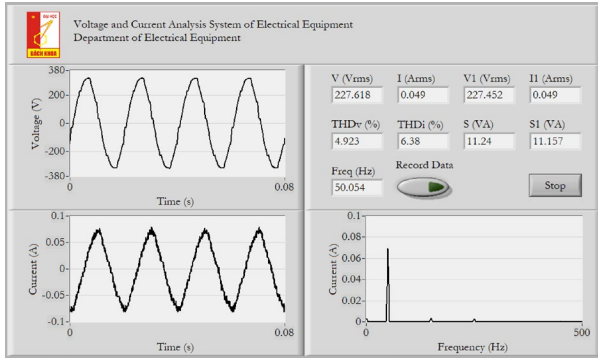


Fig. 3. GUI of the DAQ software

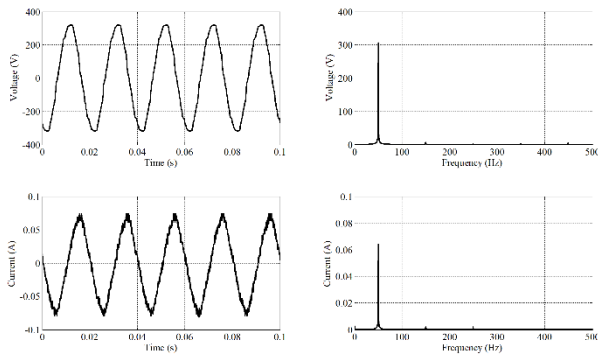


Fig. 4. Waveforms and FFT analyses of the coil voltage and current with an applied voltage of 220 V

The real power of the coil is computed as follows:

$$P = \frac{1}{N} \sum_{i=1}^N V_i I_i \quad (28)$$

The appearance power of the coil is given by:

$$S = V_{RMS} I_{RMS} \quad (29)$$

The resistance of the coil is calculated as follows:

$$R = \frac{P}{I_{RMS}^2} \quad (30)$$

The impedance of the coil is given by:

$$Z = \frac{V_{RMS}}{I_{RMS}} \quad (31)$$

The reactance of the coil is computed as follows:

$$X = \sqrt{Z^2 - R^2} \quad (32)$$

The electromagnetic force that attracts the armature can be accurately computed using finite element analysis (FEA). It directly depends on the following parameters:

- Number of turns of the coil,
- Air-gap length,
- Current flowing through the coil.

Fig. 5 illustrates the implementation of FEMM to perform a 2D finite element analysis of the AC contactor coil and its magnetic structure. In this simulation, the magnetic field distribution and magnetic flux density are computed based on the applied coil excitation, the material properties, and the geometry of the magnetic circuit. By examining these results, the influence of coil current, air-gap length, and material saturation on the overall magnetic behavior can be clearly evaluated. This provides a reliable basis for modeling the pull-in force, estimating performance under different operating conditions, and supporting design optimization of the contactor.

Fig. 6 demonstrates the learning principle of BNN, showing how weights and biases are iteratively updated during training. This probabilistic update process enables the network to learn the mapping between inputs and outputs while quantifying the uncertainty associated with each prediction.

Fig. 7 presents the methodology for generating the BNN training dataset using FEMM simulations. The electromagnetic analysis results are systematically extracted to create input–output samples, which serve as the training data for the BNN. This establishes a direct link between finite element modeling and data-driven prediction, ensuring that the neural network reflects realistic electromagnetic behavior of the AC contactor.

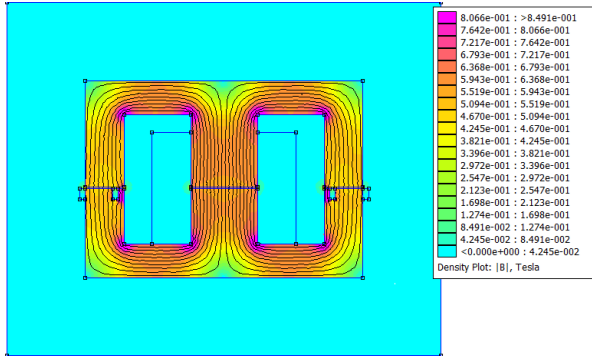


Fig. 5. 2D FEM analysis of the AC contactor

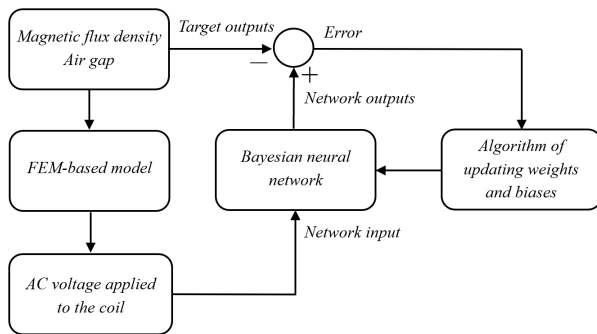


Fig. 6. Principle for updating the weights and biases of the BNN

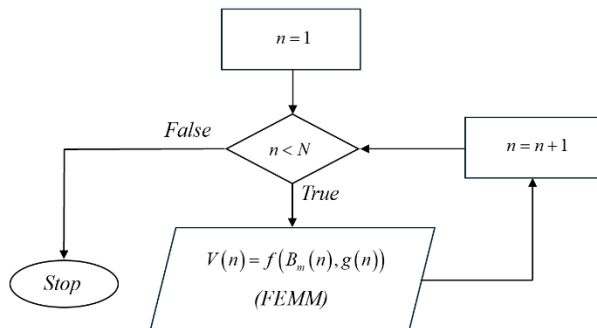


Fig. 7. Principle for generating the training data for the BNN

The BNN, which provides a mapping from the voltage applied to the coil to the corresponding flux density and air-gap length, has the following architecture:

- One input corresponding to the voltage applied to the coil,
- Ten hidden units in the hidden layer,
- Two outputs, corresponding to the flux density and air-gap length.

The network training procedure was then implemented as follows:

- **Step 1:** Choosing initial values for the hyperparameters, β and α . Initializing the values for weights and biases.
- **Step 2:** Training the network using scaled conjugate gradient optimization algorithm to minimize the cost function, S .
- **Step 3:** When the cost function has reached a local minimum, re-estimating the values of β and α using (24) and (25).
- **Step 4:** Repeating Step 2 and 3 until convergence (the cost function will not change significantly in subsequent iterations).

Table 1 presents the evolution of the hyperparameters across five consecutive re-estimation periods during the BNN training process. These updates demonstrate how the model parameters are iteratively adjusted as additional information from the training data is incorporated. By continuously refining the hyperparameters, the BNN updates the posterior distributions of its weights and biases, allowing the model to more accurately represent the underlying uncertainty in the data. This adaptive optimization process leads to improved prediction accuracy, better generalization to unseen samples, and more credible uncertainty estimates for the predicted electromagnetic quantities of the AC contactor system.

Based on the trained BNN model, the magnetic flux density and air-gap length can be estimated as functions of the voltage applied to the coil, as summarized in Table 2. This enables direct mapping from measurable electrical inputs to key electromagnetic parameters, facilitating real-time assessment of the contactor's behavior. Furthermore, by combining the FEM-based model with the applied voltage values, the operational parameters of the coil in the energized states, such as coil current, magnetic force, and flux distribution, can be accurately determined, as presented in Table 3. This integrated approach allows for a comprehensive understanding of the AC contactor's performance under different operating conditions, supporting both analysis and design optimization.

Table 1. Changes in hyperparameters across re-estimation periods

Re-estimation period	β	α
1	0.992	85.045
2	2.620	98.624
3	3.875	94.789
4	4.570	92.401
5	4.783	91.644

Table 2. Flux density and air-gap length corresponding to the voltage applied to the coil

$V_{coil} (V_{RMS})$	$B_m (T)$	$g (mm)$
160	1.4141	0.2527
170	1.3914	0.2436
180	1.3692	0.2360
190	1.3477	0.2295
200	1.3273	0.2239
210	1.3083	0.2187
227	1.2909	0.2138

Table 3. Operational parameters of the coil in the energized state

$V_{coil} (V_{RMS})$	$I_{coil} (A_{RMS})$	$B_m (T)$	$g (mm)$
227.1312	0.048	1.2373	0.2575

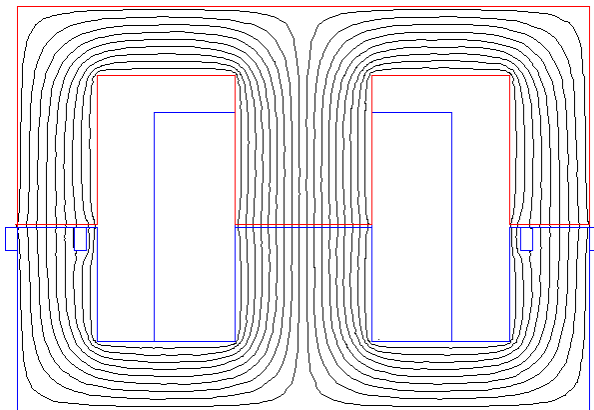


Fig. 8. Contour (red lines) used for computing the force acting on the armature core

Fig. 8 illustrates the contour lines (highlighted in red) that define the integration path used to compute the electromagnetic force acting on the armature core. These contours are applied in the FEM analysis to evaluate the magnetic field distribution around the core and determine the resulting force through the Maxwell stress tensor.

Table 4 presents the calculated electromagnetic force values in the energized state of the AC contactor coil, including the minimum, maximum, and mean force obtained from both analytical and FEM methods. These values illustrate the magnitude and range of the force acting on the armature under steady conditions, providing a quantitative basis for evaluating the contactor’s pull-in capability, mechanical stability, and operational reliability.

Table 4. Electromagnetic force values in the energized state computed by the analytical method and FEM

Force (N)	Analytical	FEM	Error (%)
F_{min}	2.2107	3.3288	33
F_{max}	47.8992	46.7812	2.39
F_{mean}	25.1119	25.0550	0.23

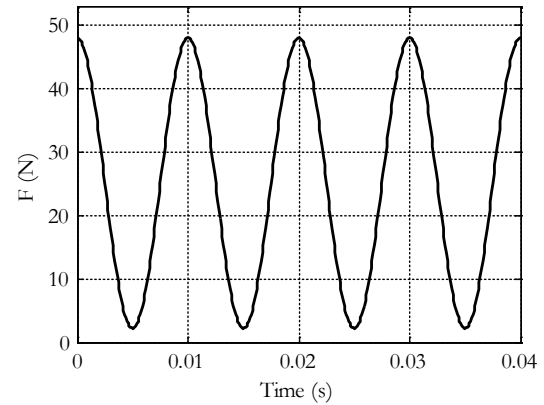


Fig. 9. Instantaneous electromagnetic force in the energized state

Fig. 9 shows the waveform of the instantaneous electromagnetic force during coil energization. The plot highlights how the force evolves over time, capturing transient fluctuations before the system reaches steady operation. This time-domain representation enables further analysis of the influence of the voltage waveform, transient dynamics, and possible force variations that may affect the contactor’s mechanical response.

Determining the energized state operating point of an AC contactor coil using a BNN provides a powerful tool for optimal electromagnet design. The energized operating point, characterized by flux density, air-gap length, and electromagnetic force, is essential for sizing the magnetic core, selecting coil parameters, and ensuring sufficient pull-in force without excessive losses or saturation. By learning the relationship between coil excitation and magnetic response, the BNN offers fast and accurate predictions that eliminate repeated FEM simulations and reduce reliance on physical prototypes. Moreover, by quantifying prediction uncertainty, the BNN helps designers evaluate safety margins, consider manufacturing tolerances, and avoid overdesign. Since the model relies on easily measured electrical signals rather than intrusive magnetic sensing, it supports cost-effective design validation and can be extended to real-time evaluation during prototyping. As a result, this approach enables more reliable, efficient, and optimized electromagnet designs with shorter development cycles and lower implementation costs.

7. Conclusion

This study has presented a computational approach for determining the energized operating point of an AC contactor coil by integrating FEM with a BNN model. The proposed method effectively estimates the magnetic flux density and air-gap length, which are key parameters significantly influencing the electromagnetic force and overall performance of the contactor. The results demonstrate that the BNN can accurately predict the internal electromagnetic quantities of the contactor, enabling precise computation of the electromagnetic attraction force through FEM analysis. This integrated FEM-BNN framework provides an efficient and reliable tool for analyzing and optimizing the operating characteristics of AC contactors, offering valuable insights for improved design and performance evaluation in industrial applications.

Acknowledgments

This research is funded by Hanoi University of Science and Technology (HUST) under project number T2024-PC-059.

References

- [1] Li, Kui, Chengchen Zhao, Feng Niu, Shumei Zheng, Yu Duan, Shaopo Huang, and Yi Wu, Electrical performance degradation model and residual electrical life prediction for AC contactor, in *IEEE Transactions on Components, Packaging and Manufacturing Technology*, vol. 10, iss. 3, pp. 400–417, March 2020, <https://doi.org/10.1109/TCPMT.2020.2966516>
- [2] S. Sun, Q. Wang, T. Du, J. Wang, S. Li, and J. Zong, Quantitative evaluation of electrical life of AC contactor based on initial characteristic parameters, in *IEEE Transactions on Instrumentation and Measurement*, vol. 70, pp. 1–10, 2021, Art. no. 3503510, <https://doi.org/10.1109/TIM.2020.3031160>
- [3] Z. Zheng, W. Ren, and T. Wang, Experimental investigation of the breaking Arc behavior and interruption mechanisms for AC contactors, in *IEEE Transactions on Plasma Science*, vol. 49, iss. 1, pp. 389–395, Jan. 2021, <https://doi.org/10.1109/TPS.2020.3042545>
- [4] R. Gollee and A. Gerlach, An FEM-based method for analysis of the dynamic behavior of AC contactors, in *IEEE Transactions on Magnetics*, vol. 36, iss. 4, pp. 1337–1340, July 2000, <https://doi.org/10.1109/20.877686>
- [5] Z. Wu, C. Fang, G. Wu, Z. Lin, and W. Chen, A CNN-regression-based contact erosion measurement method for AC contactors, in *IEEE Transactions on Instrumentation and Measurement*, vol. 71, pp. 1–10, 2022, Art. no. 3518410, <https://doi.org/10.1109/TIM.2022.3192282>
- [6] T. Longfei, X. Zhihong, and B. Venkatesh, Contactor modeling technology based on an artificial neural network, in *IEEE Transactions on Magnetics*, vol. 54, no. 2, pp. 1–8, Feb. 2018, Art. no. 4900108, <https://doi.org/10.1109/TMAG.2017.2767555>
- [7] Ian Nabney. *NETLAB: Algorithms for Pattern Recognition*. Springer London, 2002.
- [8] D. Meeker. *Finite Element Method Magnetics (FEMM) User's Manual*. Version 4.2. 2017.
- [9] M. F. Møller, A scaled conjugate gradient algorithm for fast supervised learning, *Neural Networks*, vol. 6, iss. 4, pp. 525–533, 1993.